

**DFTB APPROACH TO MULTIPLY CHARGED Au^{q+}_n CLUSTERS
PART I-STRUCTURAL AND ELECTRONIC PROPERTIES**

Nathalie Tarrat^{1,a}, Mathias Rapacioli^{2,b}, Bishal Poudel², Fernand Spiegelman²

¹ CEMES, CNRS, Université de Toulouse, 29 Rue Jeanne Marvig, 31055 Toulouse, France

² Laboratoire de Chimie et Physique Quantiques LCPQ/FeRMI, UMR 5626, Université de Toulouse (UPS) and CNRS, 118 Route de Narbonne, F-31062 Toulouse, France

Corresponding author: ^a nathalie.tarrat@cemes.fr; ^b rapacioli@irsamc.ups-tlse.fr

[§] Dedicated to J. Christian Schön on the occasion of his 66th birthday

Abstract: *This series of two papers reports the investigation of the properties of multiply charged gold clusters cations Au^{q+}_n (n = 3 – 20) up to charge q = 4. In the present part I of the study, a global exploration of their potential energy surface has been performed using a combination of parallel tempering molecular dynamics and quenches performed at the DFTB level. When increasing the charge of the clusters, their structure was found to evolve from a compact form to an elongated one, shifting the 2D/3D transition toward larger sizes. Such structure elongation is explained by the minimization of coulombic destabilization. In the further part II of this study, the stability of these low-energy isomers will be discussed, with a focus on the cluster's ionization and fragmentation.*

Keywords: gold, multiply charged clusters, PTMD, DFTB

1. Introduction

Gold clusters and nanoparticles have been the focus of wide interest. Indeed, due to relativistic effects and despite the fact that they have only one electron in the outer *s* shell, they offer electronic properties rather different from the other monovalent metal clusters, in terms of structure, bonding, electronic spectroscopy, or reactivity. The structure of neutral and singly charged anionic and cationic gold clusters has been the subject of numerous investigations, experimentally [1–5] and theoretically [1,5–17.] In contrast, while stability and fragmentation of multiply charged gold clusters could be studied via the liquid drop model [18–19], only a few publications have dealt with their actual atomistic structure [20–23], although charge is expected to play a strong role in their spectroscopic and chemical properties. In the present work, we investigate systematically the structural and energetic properties of gold cluster cations Au^{q+}_n with n = 3 – 20 and q = 1 – 4.

Part I (present paper) is dedicated to the investigation of structural properties of multiply charged gold clusters using the Density Functional-based Tight Binding (DFTB) method and a global optimization scheme, while Part II will discuss the energetical outcomes. The goals are multi-fold: (i) achieve a systematic study of multiply charged gold cluster cations up to 20 atoms, where electronic structure, cluster charge, and geometrical structure are mostly coupled (ii) determine the energetical properties, such as stability, metastability, ionization, and fragmentation properties (iii) probe whether DFTB, initially designed to study charge fluctuation close to atomic neutrality, is able to deal with clusters from neutral to high charge states.

2. Method

Geometry optimization was conducted with a global algorithm, namely (i) Parallel tempering molecular dynamics (PTMD) [24] involving replica exchanges of configurations between trajectories ran at different temperatures, according to the Metropolis criterion [25] (ii) selecting configurations obtained at regular intervals along the trajectories at chosen temperatures (iii) quenches of those configurations via a conjugated-gradient driven descent to the local minima (iv) identifying and ordering the various minima structures according to their energies in order to find the most stable ones.

The PTMD sampling was conducted with zeroth-order DFTB [26]. Oppositely, the quenches were made using second-order DFTB [27-28], the parameters published in our previous work [25] and modified on-site integrals (0.42, 0.255, 0.255 for U_d , U_p , and U_s). The theoretical gold atom successive ionization potentials are 9.21, 21.15, 32.57, 44.00, and 58.09 eV, in good agreement with the experimental values (experimental uncertainty between parentheses) of 9.225 (0.00), 20.20 (0.02), 30.00 (1.61), 45 (1.74) and 60.00 (1.86) eV [29]. The PTMD runs involved 60 temperatures between 50 and 3000 K with classical MD propagation coupled to a chain of 5 Nose-Hoover thermostats with a unique frequency of 80 cm^{-1} . The trajectories were propagated during 10^6 timesteps of 3 fs at each temperature. Exchanges were attempted every 100 time steps. Finally, about 250 configurations were extracted along 6 trajectories (namely at 93, 187, 374, 529, 749, 1059, and 1499 K) and quenched towards their local minimum. Note that the melting temperature of gold bulk is 1337 K [30]. It may be that PTMD simulations fail to produce long extension chains or ribbons. Thus we have specially investigated low-dimensional clusters such as chains, chains with triangle or rhombus terminations, or nanoribbons, which were included in the final energy-based isomers ordering. The calculations have been performed with deMonNano and DFTB+ softwares [31-32].

3. Results and discussion

We first address the structural properties of neutral gold clusters Au_n which have been widely investigated in the literature and in our previous works. Small gold clusters are known to present non-linear planar shapes. This appetite for 2D structures results from relativistic effects and was shown to be fairly reproduced by DFTB [25–33]. 2D structures are more stable than 3D up to 6 atoms, 2D and 3D structures are almost degenerate between 7 and 11 atoms and 3D structures are more stable above this size. Our previous work was limited to sizes up to 13 units and to size 20 [25–34], and has been extended in the present work to clusters from 14 to 19 units as shown in Figure 1 where the most and second most stable isomers are labeled with "a" and "b" letters. These clusters present 3D compact structures with either disordered shapes (see for instance 15a or 16a) or symmetric geometries (see for instance 17a, or 19a which can be seen as deriving from the Au_{20} pyramidal structure with the removal of a vertex atom). The global minimum of Au_{14} (14a) is similar to the one reported by Chaves et al. [13] by implementing a systematic study performed at the spin-polarized symmetry-unrestricted DFT level but this is not the case for Au_{15} for which the structure they reported is more symmetrical. Using a combination of DFTB and an unbiased modified basin hopping optimization algorithm, Yen et al. reported non-symmetric structures for all sizes from Au_{14} to Au_{18} [12], which only differs from our results in the case of Au_{14} and Au_{17} for which 14a and 17a are symmetrical. In the case of Au_{19} , our results are consistent, the lowest energy structure being a pyramid with one of its vertex cut off. An interesting point to note, in connection with the study reported by Nhat et al. showing that Au_{18} can form cages [17], is that our third low-energy Au_{18} isomer is a hollow one, separated from the most stable one by only 0.06 meV.

In the case of the monocationic gold clusters Au^{q+}_n , the 2D-3D transition is more marked than for the neutrals, between 7 and 8 units, as can be seen in Figure 2, without 2D-3D competition for the larger

sizes. For these latter, either disordered or symmetric structures can be observed. The results of our exploration can be compared with the one of Fernandez et al. [16], which reports a DFT study for clusters up to Au^+_{13} , by exploring a limited number of initial structures. Our lowest energy isomer is generally consistent with a few examples in which our second isomer is found to be their most stable one or the opposite (e.g. Au^+_{5} , Au^+_{8} , and Au^+_{12}), possibly combined with an adatom on a different place on the cluster (Au^+_{11}). In the case of Au^+_{13} they find our most stable isomer at higher energy, with an adatom at a different position. The structure of these isomers has also been studied by Gilb et al. [1] by combining ion mobility measurements and molecular dynamics followed by several dozen quenches to explore different candidate topologies at the DFT level. The global minima found are in agreement with ours up to size 12 with, as in the previous case, some examples for which our most stable isomer is their second isomer (Au^+_{8} and Au^+_{10}) or the opposite (Au^+_{9}). These differences most likely come from the use of different energy functions because in the case of size 8 we have also found their structures during our exploration but not in the same energetic order. At size 13, our two studies find symmetrical but different lowest energy isomers. The structure of isomers of sizes 3 to 11 has been more recently studied by Gao et al. [11] at the DFT level by conducting global exploration with the global reaction route mapping technique combined with the anharmonic downward distortion following and the artificial force-induced reaction methods. The only difference with our results concerns Au^+_{8} for which their lowest energy isomer is found in the fifth position of our exploration. Schooss et al. studied a wider size range and reported on the structure of Au^+_n with n in the range 3-20, by implementing a DFT-based genetic algorithm for sizes 14 to 19^2 . For all the small sizes up to 12 and size 20, our results agree, with a slight difference for size 9, where the isomer we found to be the most stable is their second isomer. For size 13, the structure reported by Schooss et al. is symmetrical but slightly different from 13a. For sizes 14 to 19, our results differ, with overall more symmetrical structures found in their study. Finding symmetrical systems only may come from the use of genetic algorithms in which the exploration of disordered isomers proves complicated when the generations of parents are mainly symmetrical. Certain studies in the literature have focused no longer on size ranges but on specific sizes, such as that of Förstel et al. which explores the case of Au^+_4 , on the basis of a vibronic optical photodissociation spectrum, and concludes that the Y-shaped isomer (C_{2v}) is the most stable, and not the rhombic one (D_{2h}) [4]. Our exploration finds these two isomers to be totally degenerate (the energy difference being of the order of a hundredth of a meV). In the case of Au^+_9 , Attia et al. [23] have also obtained a pyramid with one of its vertex cut off at the DFT level from a very limited number of polyhedra explored. At size 17, our most stable structure corresponds to the one reported by Yan et al. [10], on the basis of an unbiased global exploration of the potential energy surface using a genetic algorithm at the DFT level, composed of an Au_{13} octahedral core with an adatom on four of its triangular faces. By comparing all these studies, we therefore observe that overall the isomers found are similar, but that the hierarchy sometimes varies. This is due to the fact that these isomers are all in a very small energy range and consequently the relative order between them is very difficult to determine, as shown by the study of the dependence of isomer order on the DFT functional reported by Walker et al. [7].

In the case of dicationic gold clusters Au^{2+}_n , the situation is slightly different because the charge on the cluster is such that structures allowing some distance between the charges start to be favored (see Figure 3). First, the trimer is more stable as a linear chain and not as a triangle, and the tetramer is a 3D-tetrahedron. 4, 5, 6, and 8 units clusters present planar shapes whereas for the heptamer, a 3D structure consisting of a triangle plus an out of plan atom starts to compete with the planar one (global minimum). For 9, 10, and 11 sizes, the most stable isomers correspond to pyramidal-based structures, whereas Au^{2+}_{20}

does not maintain anymore a pyramidal structure. The structures of sizes 14, 15, and 18 are found to be symmetrical whereas they were not for the clusters carrying a single charge. In the literature, knowledge relating to the structure of dicationic gold clusters is very incomplete. In a study focused on spherical aromaticity, Petrar et al. have explored the structure of Au^{2+}_{10} by comparing the DFT energy of ten polyhedra and concluded that the lowest isomer has a symmetrical tetrahedral geometry [21], in agreement with our global minimum at this size.

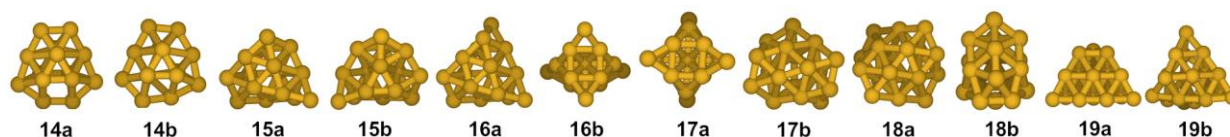


Figure 1. Geometries of the lowest and second lowest energy isomers of Au_n ($n = 14 - 19$).

Tricationic gold clusters Au^{3+}_n with less than 4 units are not stable, and tetra and pentamer most stable clusters are made of a single chain as can be seen in Figure 4. The most stable clusters of up to 8 units present an elongated shape, often presenting a group of 4 atoms at their tips. The most stable structures of clusters with 9, 10, and 12 units are still planar but more compact whereas the clusters with 11 and more than 12 units are clearly 3 dimensional, the 2D form of Au^{3+}_{11} lying 347 meV above its global minimum. For larger sizes, the global minimum structures turn out to be quite ordered, even symmetrical (13a, 14a, 15a, 18a) except at size 20 where a disorderly character appears. One can compare our data with the literature at size 11 as Attia et al. developed a study of cationic gold clusters with eight valence electrons [23], in which they found a global minimum for Au^{3+}_{11} more compact than ours, which exhibits an adatom. However, all the candidates they explored, seven in number, were compact structures. We have also found compact forms but at much higher energies, probably as they imply destabilizing close proximity of charges.

The most stable structures for gold clusters carrying 4 positives charges Au^{4+}_n are reported in Figure 5. Clusters with less than 6 units did not remain stable. For clusters up to 19 units, the charge repulsion led to elongated structures as the first or second most stable minimum except in the case of Au^{4+}_{18} . These elongated structures can be classified as linear chains (e.g. 6a, 7a, 8a), linear chains with a final 3- or 4-atom planar island (e.g. 9a, 10a, 11a, 12a, 13a, 14a), or nanoribbons (e.g. 15a, 17a, 19a). Finally, Au^{4+}_{20} has completely lost its pyramidal based structure with a very disordered shape. Attia et al. have explored 15 structures of Au^{4+}_{12} and found a compact lowest-energy isomer [23]. But as for the tricationic cluster Au^{3+}_{11} their exploration was focused on compact Au^{4+}_{12} . In such compact geometries, the charges can not be as far apart as in the case of the elongated structure shown in Figure 5.

To develop our assumption that structures tend to elongate as their charge increases to allow a spatial distance between the charges, we show in Figure 6 the Mulliken charges distribution of three clusters, Au^{2+}_{10} , Au^{4+}_{10} , and Au^{4+}_{19} . This electronic density analysis confirms that the charge is mostly carried by few atoms or groups of atoms localized as far as possible from each other to minimize coulomb repulsion. For instance, charge accumulations are observed on the vertex atoms of pyramidal-based structures (Au^{2+}_{10}), on the tip atoms in the nanoribbons (Au^{4+}_{19}), or on the triangular end groups of the chain structures (Au^{4+}_{10}). Maximizing the distance between the charged groups thus explains the shift of the 2D/3D transition toward larger sizes when the charge increases. Our results can be compared with

those of Manzoo et al. on the Au^+_6 cluster which reports DFT charges on the vertex atoms of the triangle (0.25, 0.27, and 0.32) [9] of comparable amplitude to our DFTB ones (0.22, 0.22, and 0.29).

4. Conclusion

We have performed a global exploration of the DFTB potential energy surfaces of neutral, singly, and multiply charged gold clusters Au^{q+}_n ($n = 3 - 20$, $q = 0 - 4$). The results are in general good agreement with previous theoretical data of the literature, mainly conducted with DFT on neutral and singly charged clusters. We have shown that, when the charge increases, the gold cluster structures evolve from a compact form to an elongated one, shifting the 2D/3D transition to larger sizes. This elongation of the structures allows to minimize coulombic destabilization. The energy behavior and stability of these low-energy isomers will be reported and discussed in part II of this study, with a focus on the cluster's ionization and fragmentation. We will show in particular that the small clusters at charge $q = 2$ and all clusters at charges $q = 3$ and $q = 4$ are metastable.

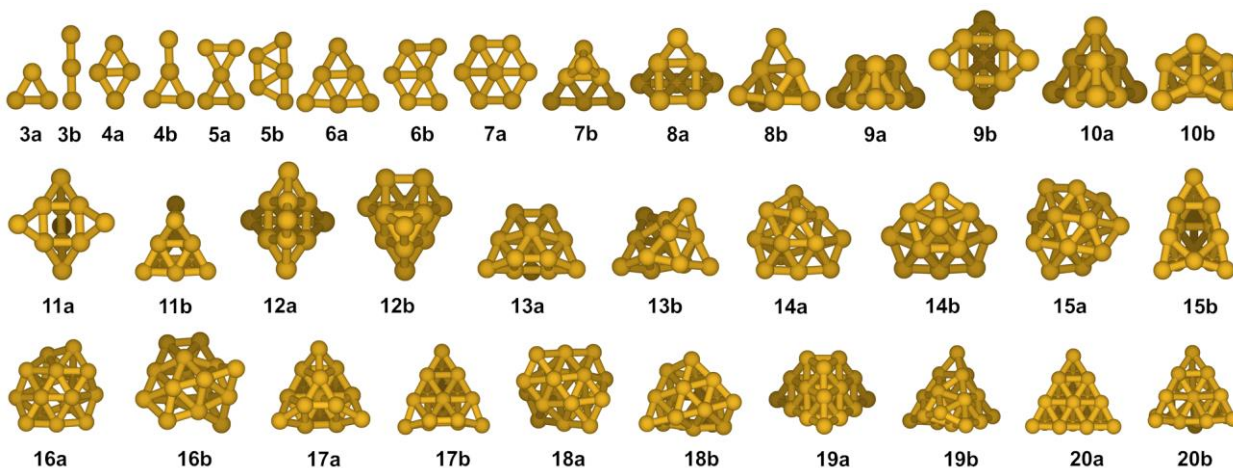


Figure 2. Geometries of the lowest and second lowest energy isomers of Au^+_n ($n = 3 - 20$).

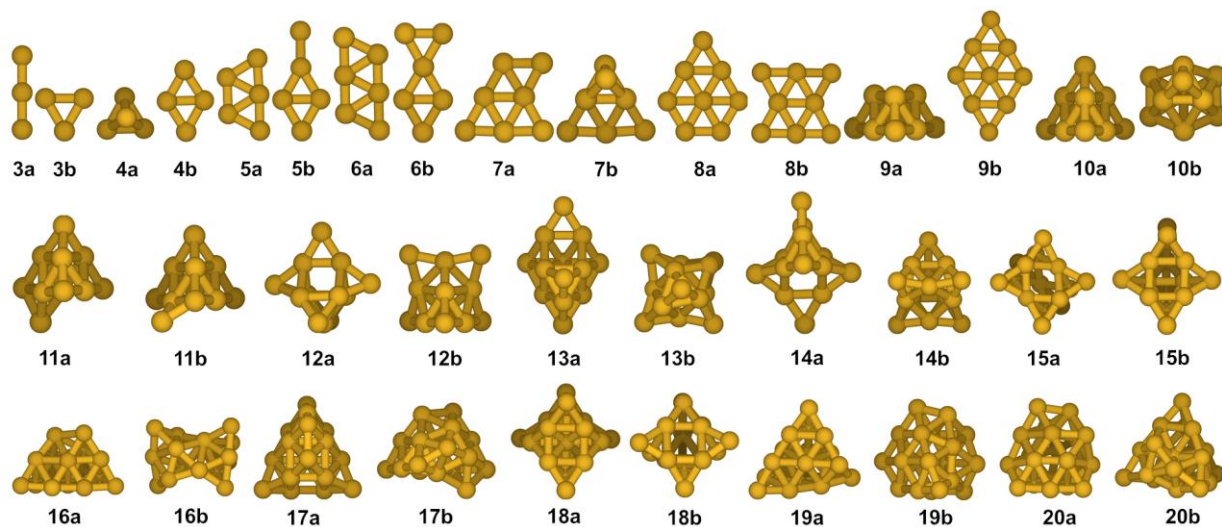


Figure 3. Geometries of the lowest and second lowest energy isomers of Au^{2+}_n ($n = 3 - 20$).

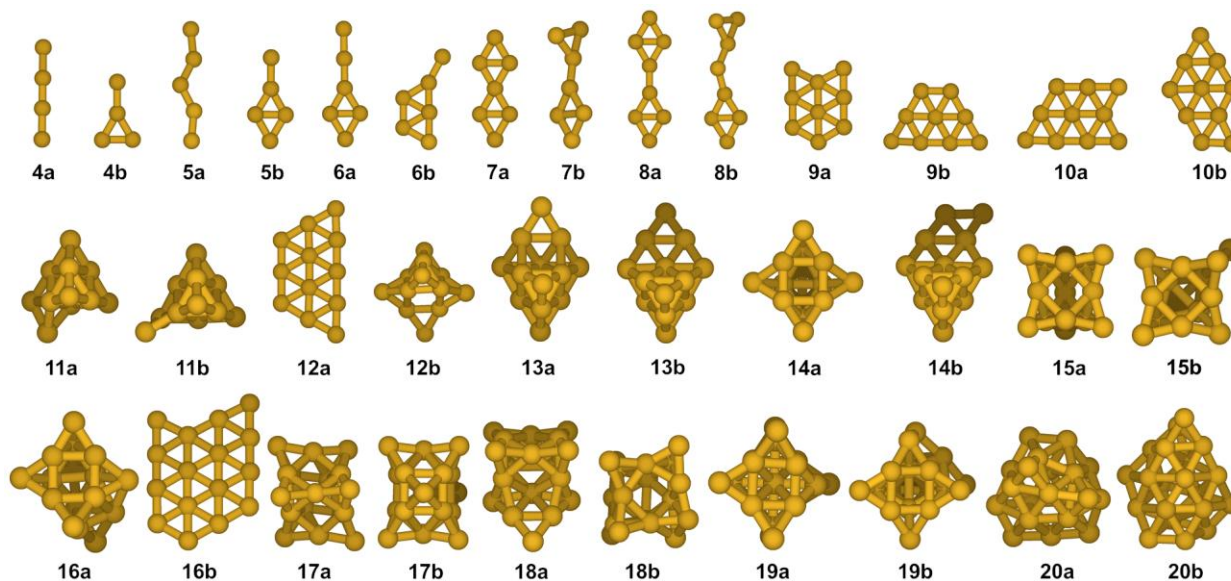


Figure 4. Geometries of the lowest and second lowest energy isomers of Au^{3+}_n ($n = 4 - 20$).

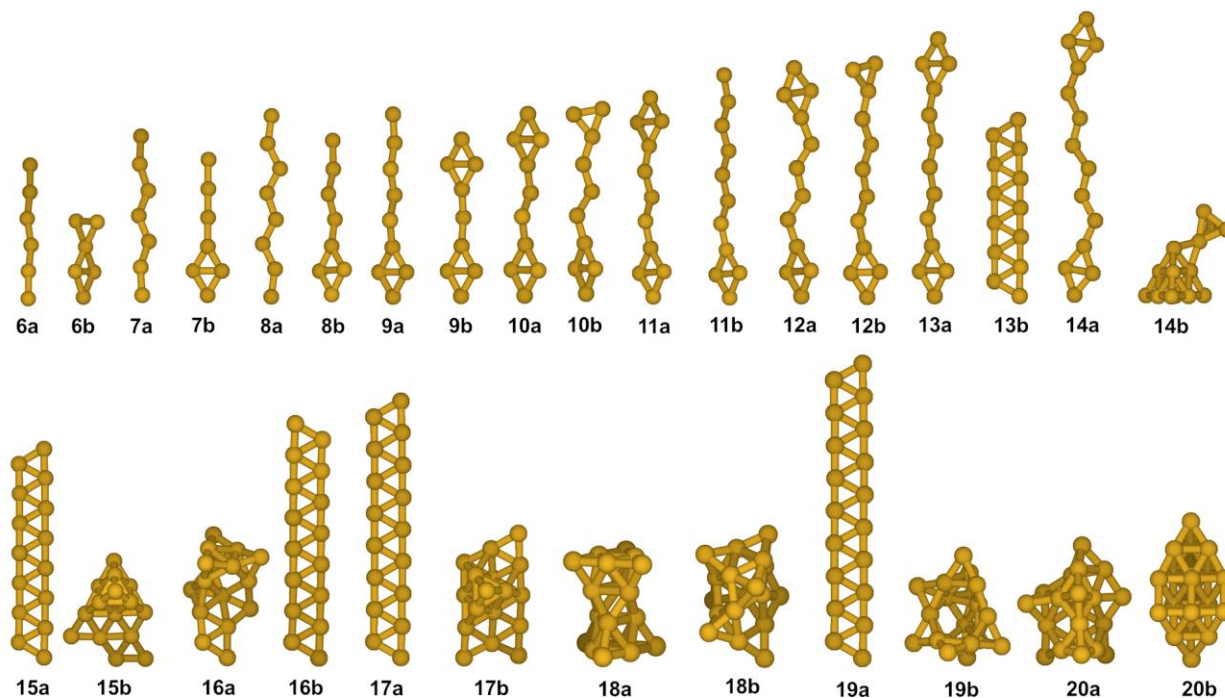


Figure 5. Geometries of the lowest and second lowest energy isomers of Au^{4+}_n ($n = 6 - 20$).

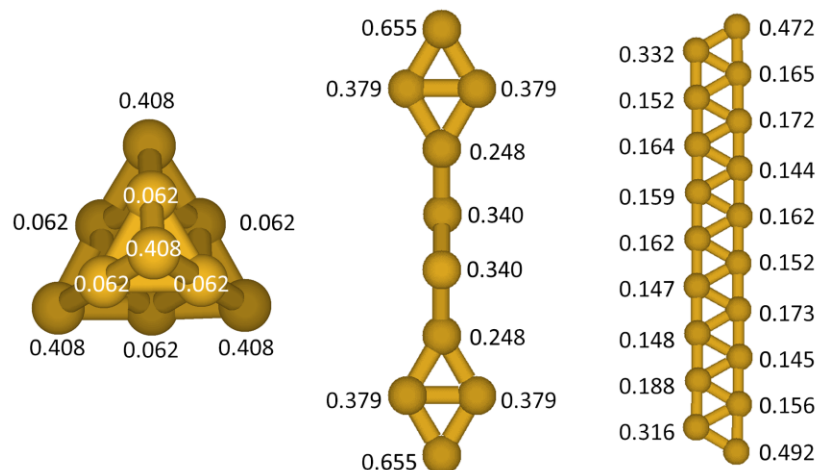


Figure 6. Mulliken atomic charges of Au^{2+}_{10} (left), Au^{4+}_{10} (middle) and Au^{4+}_{19} (right).

Acknowledgments

This work was granted access to the HPC resources of CALMIP supercomputing center under the allocations p0059, p18009, and p1303

References

- [1] S. Gilb, P. Weis, F. Furche, R. Ahlrichs, and M. M. Kappes, *J. Chem. Phys.* 116, 4094 (2002).
- [2] D. Schooss, P. Weis, O. Hampe, and M. M. Kappes, *Philos. Trans. Royal Soc.* 368, 1211 (2010).
- [3] A. P. Woodham and A. Fielicke, "Gold clusters in the gas phase," in *Gold Clusters, Colloids and Nanoparticles I*, edited by D. M. P. Mingos (Springer International Publishing, Cham, 2014) pp. 243–278.
- [4] M. Forstel, W. Schewe, and O. Dopfer, *Angew. Chem. Int. Ed.* 58, 3356 (2019).
- [5] P. Ferrari and E. Janssens, *Molecules* 26 (2021).
- [6] E. M. Fernández, J. M. Soler, I. L. Garzón, and L. C. Balbás, *Phys. Rev. B* 70, 165403 (2004).
- [7] A. V. Walker, *J. Chem. Phys.* 122, 094310 (2005).
- [8] H. Hakkinen, *Chem. Soc. Rev.* 37, 1847 (2008).
- [9] D. Manzoor, S. Pal, and S. Krishnamurty, *J. Phys. Chem. C* 117, 20982 (2013).
- [10] L. Yan, L. Cheng, and J. Yang, *J. Phys. Chem. C* 119, 23274 (2015).
- [11] M. Gao, A. Lyalin, M. Takagi, S. Maeda, and T. Taketsugu, *J. Phys. Chem. C* 119, 11120 (2015).
- [12] T.-W. Yen, T.-L. Lim, T.-L. Yoon, and S. Lai, *Comput. Phys. Commun.* 220, 143 (2017).
- [13] A. S. Chaves, M. J. Piotrowski, and J. L. F. Da Silva, *Phys. Chem. Chem. Phys.* 19, 15484 (2017).
- [14] F. Baletto, *J. Phys. Condens. Matter.* 31, 113001 (2019).
- [15] B. R. Goldsmith, J. Florian, J.-X. Liu, P. Gruene, J. T. Lyon, D. M. Rayner, A. Fielicke, M. Scheffler, and L. M. Ghiringhelli, *Phys. Rev. Mater.* 3, 016002 (2019).
- [16] S. K. Lai and C. C. Lim, *J. Comput. Chem.* 42, 310 (2021).
- [17] P. V. Nhat, N. T. Si, A. Fielicke, V. G. Kiselev, and M. T. Nguyen, *Phys. Chem. Chem. Phys.* 25, 9036 (2023).
- [18] W. A. Saunders, *Phys. Rev. Lett.* 64, 3046 (1990).
- [19] U. Naher, S. Bjornholm, S. Frauendorf, F. Garcias, and C. Guet, *Physics Reports* 285, 245 (1997).
- [20] B. Molina, J. Soto, and A. Calles, *Eur. Phys. J. D* 51, 225 (2009).
- [21] P. M. Petrar, M. B. Sárosi, and R. B. King, *J. Phys. Chem. Letters* 3, 3335 (2012).
- [22] A. Held, M. Moseler, and M. Walter, *Phys. Rev. B* 87, 045411 (2013).
- [23] A. A. A. Attia, A. M. V. Branzanic, A. Muñoz Castro, A. Lupan, and R. B. King, *Phys. Chem. Chem. Phys.* 21, 17779 (2019).
- [24] Y. Sugita and Y. Okamoto, *Chem. Phys. Lett.* 314, 141 (1999).
- [25] L. F. L. Oliveira, N. Tarrat, J. Cuny, J. Morillo, D. Lemoine, F. Spiegelman, and M. Rapacioli, *J. Phys. Chem. A* 120, 8469 (2016).
- [26] D. Porezag, T. Frauenheim, T. Köhler, G. Seifert, and R. Kaschner, *Phys. Rev. B* 51, 12947 (1995).
- [27] M. Elstner, D. Porezag, G. Seifert, T. Frauenheim, and S. Suhai, *MRS Proceedings* 538, 541.

- [28] F. Spiegelman, N. Tarrat, J. Cuny, L. Dontot, E. Posenitskiy, C. Mart'ı, A. Simon, and M. Rapacioli, *Advances in Physics: X*, *Advances in Physics: X* 5, 1710252 (2020).
- [29] A. Kramida, Y. Ralchenko, J. Reader, and N. A. Team, NIST Atomic Spectra Database (ver. 5.10), [Online]. Available: <https://physics.nist.gov/asd> [2023, November 24]. National Institute of Standards and Technology, Gaithersburg, MD. (2022).
- [30] G. Kaye and T. Laby, *Tables of Physical and Chemical Constants* 15th ed. (Longman, London, UK, 1993).
- [31] M. Rapacioli, T. Heine, L. Dontot, M. Yusef Buey, E. Posenitskiy, N. Tarrat, F. Spiegelman, F. Louisnard, C. Marti, J. Cuny, M. Morinire, C. Dubosq, S. Patchkovskii, J. Frenzel, E. Michoulier, H. Duarte, L. Zchekhov, and D. Salahub, “deMonNano, <http://demon-nano.ups-tlse.fr/>,” (2023).
- [32] B. Aradi, B. Hourahine, and T. Frauenheim, *J. Phys. Chem. A* 111, 5678 (2007).
- [33] J. Cuny, N. Tarrat, F. Spiegelman, A. Huguenot, and M. Rapacioli, *Journal of Physics: Condensed Matter* 30, 303001 (2018). 34N. Tarrat, M. Rapacioli, J. Cuny, J. Morillo, J.-L. Heully, and F. Spiegelman, *Comput. Theor. Chem.* 1107, 102 (2017).